



Available online at www.sciencedirect.com

ScienceDirect

journal homepage: www.e-jmii.com



Original Article

Metal nanoparticles and nanoparticle composites are effective against *Haemophilus influenzae*, *Streptococcus pneumoniae*, and multidrug-resistant bacteria

Yu-Shan Huang^{a,b}, Jann-Tay Wang^{a,c,*}, Hui-Ming Tai^d,
Pai-Chun Chang^e, Hsin-Chang Huang^e, Pan-Chyr Yang^{a,f}



^a Department of Internal Medicine, National Taiwan University Hospital, Taipei, Taiwan

^b Graduate Institute of Clinical Medicine, National Taiwan University College of Medicine, Taipei, Taiwan

^c National Institute of Infectious Diseases and Vaccinology, National Health Research Institutes, Miaoli, Taiwan

^d Laboratory of Infectious Disease, Department of Internal Medicine, National Taiwan University Hospital, Taipei, Taiwan

^e Tripod Nano Technology Corporation, Taoyuan, Taiwan

^f Institute of Biomedical Sciences, Academia Sinica, Taipei, Taiwan

Received 23 January 2022; received in revised form 26 April 2022; accepted 26 May 2022

Available online 9 June 2022

KEYWORDS

Respiratory infections;
Metal nanoparticles;
Multidrug-resistant organisms;
Antibacterial therapy

Abstract *Background:* Treatment for lower respiratory tract infection caused by multidrug-resistant organisms (MDRO) are often limited. This study explored the activity of different metal nanoparticles against several respiratory pathogens including MDROs.

Methods: Clinical isolates of carbapenem-resistant *Acinetobacter baumannii* (CRAB), carbapenem-resistant *Klebsiella pneumoniae* (CRKP), *Pseudomonas aeruginosa*, *Haemophilus influenzae*, methicillin-resistant *Staphylococcus aureus* (MRSA), and *Streptococcus pneumoniae* were tested for *in vitro* susceptibilities to various antibiotics and nanoparticles. Minimum inhibitory concentrations (MICs) of silver-nanoparticle (Ag-NP), selenium-nanoparticle (Se-NP), and three composites solutions ND50, NK99, and TPNT1 (contained 5 ppm Ag-NP, 60 ppm ZnO-nanoparticle, and different concentrations of gold-nanoparticle or ClO₂) were determined by broth microdilution method.

* Corresponding author. Department of Internal Medicine, National Taiwan University Hospital, 7 Chung-Shan South Road, Taipei 100, Taiwan.

E-mail address: wang.jt1968@gmail.com (J.-T. Wang).

Results: Fifty isolates of each bacterial species listed above were tested. Ag-NP showed lower MICs to all species than Se-NP. The MIC₅₀s of Ag-NP for CRAB, CRKP, *P. aeruginosa*, and *H. influenzae* were <3.125 ppm, 25 ppm, <3.125 ppm, and <3.125 ppm, respectively, while those for *S. pneumoniae* and MRSA were >50 ppm and 50 ppm. Among CRAB, CRKP and *P. aeruginosa*, the MIC₅₀s of ND50, NK99, and TPNT1 for CRAB were the lowest (1/8 dilution, 1/8 dilution, and 1/8 dilution, respectively), and those for CRKP (>1/2 dilution, 1/2 dilution, and 1/2 dilution, respectively) were the highest. Both MRSA and *S. pneumoniae* showed high MIC₅₀s to ND50, NK99, and TPNT1.

Conclusions: Metal nanoparticles had good *in vitro* activity against Gram-negative bacteria. They might be suitable to be prepared as environmental disinfectants or inhaled agents to inhibit the growth of MDR Gram-negative colonizers in the lower respiratory tracts of patients with chronic lung diseases.

Copyright © 2022, Taiwan Society of Microbiology. Published by Elsevier Taiwan LLC. This is an open access article under the CC BY-NC-ND license (<http://creativecommons.org/licenses/by-nc-nd/4.0/>).

Introduction

Lower respiratory tract infection (LTI) is the leading cause of morbidity and mortality worldwide. Typical pathogens of community-acquired bacterial pneumonia include *Streptococcus pneumoniae* and *Haemophilus influenzae*.¹ Although antimicrobials substantially improved the outcomes of patients with LTI, drug-resistant pneumococcus has emerged and now become a growing concern.² Similarly, the prevalence of hospital-acquired LTI caused by multidrug-resistant organisms (MDROs) is increasing.³ Infections caused by MDRO had limited therapeutic options, and were associated with high mortality risk and medical expenses. In patients with chronic obstructive pulmonary disease or bronchiectasis, airway colonization of MDROs has been associated with more frequent exacerbation and poor outcomes.^{4,5} To combat MDRO-related infections, newer antibacterial agents are in urgent need.

MDROs such as methicillin-resistant *Staphylococcus aureus* (MRSA), carbapenem-resistant *Acinetobacter baumannii* (CRAB), or *Pseudomonas aeruginosa* can not only cause invasive infections but also colonize on human body or environmental surfaces. The transmission of MDROs can be facilitated by contaminated surfaces in the hospital,⁶ thus cleaning and disinfecting hospital environments are important components of infection control. Bacterial pathogens with decreased susceptibility to commonly used antiseptics had been reported.^{7,8} Therefore, the introduction of novel disinfectants may contribute to hospital cleanliness.

Nanoparticles are materials with a diameter of less than 100 nm, which are developed for various biological and medical applications. Metallic-based nanoparticles had been shown to trigger the release of reactive oxygen species (ROS) when contact with cell membranes, thus interfere the survival of bacteria.⁹ Prior studies showed that chitosan-capped selenium nanoparticles (Se-NP) could inhibit the growth of *Escherichia coli*, *S. aureus*, and *Candida albicans*.^{10,11} Silver nanoparticle (Ag-NP) expressed *in vitro* antibacterial activity against carbapenem-resistant *Klebsiella pneumoniae* (CRKP),¹² and gold nanoparticle (Au-NP) could suppress *Mycobacterium*

tuberculosis.¹³ The application of nanoparticles in environmental disinfection have also been investigated.¹⁴ Although many reports were published, few data compared the anti-bacterial activity of different metal nanoparticles against multidrug-resistant bacteria.

This study aimed to explore the *in vitro* antibacterial activity of colloidal Ag-NP, Se-NP, and three nanoparticles composites solutions against important pathogens of community and nosocomial pneumonia.

Methods

Collection of bacterial isolates

This study was conducted at a 2200-bed tertiary care center (National Taiwan University Hospital) in Northern Taiwan during January 2020 to July 2021. Stored clinical isolates of MRSA, *S. pneumoniae*, *H. influenzae*, *P. aeruginosa*, CRAB and CRKP collected from 2019 to 2021 were randomly selected for *in vitro* susceptibility study. All MRSA and *P. aeruginosa* were isolated from blood, and 48 (96%) of 50 CRAB were from blood. The *S. pneumoniae*, *H. influenzae*, and CRKP were isolated from various clinical specimens, which were shown in [Supplementary Table 1](#). These bacteria were cultured from clinical specimens in the microbiological laboratory at National Taiwan University Hospital. The bacteremic isolates were detected using the Bactec 9240 system (Becton Dickinson, Sparks, MD). All bacterial isolates were subjected to bacterial identification by Bruker Biotyper matrix assisted laser desorption ionization-time of flight mass spectrometry (MALDI-TOF MS) system. *Acinetobacter baumannii* isolates tested resistant to imipenem, meropenem or doripenem were defined as CRAB. *K. pneumoniae* isolates with imipenem or meropenem minimum inhibitory concentrations (MICs) ≥ 4 $\mu\text{g}/\text{mL}$ or ertapenem MIC ≥ 2 $\mu\text{g}/\text{mL}$ were defined as CRKP. Carbapenem-resistant *P. aeruginosa* (CRPA) was defined as an isolate with imipenem or meropenem MICs ≥ 8 $\mu\text{g}/\text{mL}$, and the other *P. aeruginosa* isolates were considered as carbapenem-susceptible *P. aeruginosa* (CSPA).

Formulation of metal nanoparticle composites

Five metal nanoparticle solutions including Ag-NP, Se-NP, ND50, NK99, and TPNT1 were evaluated. These nanoparticle solutions were provided by the manufacturer (Tripod Nano Technology Corp. Taoyuan, Taiwan). Ag-NP and Se-NP each contained 100 ppm colloidal Ag and Se nanoparticles dissolved in citric acid. ND50, NK99, and TPNT1 had the same composition in aqueous solution, only the ratio of nanoparticles and chlorine dioxide (ClO_2) are adjusted. ND50 contained 1 ppm Au-NP, 5 ppm Ag-NP, 60 ppm Zinc oxide nanoparticles (ZnO-NP), and 6.5 ppm ClO_2 . NK99 contained 0.1 ppm Au-NP, 5 ppm Ag-NP, and 60 ppm ZnO-NP. TPNT1 contained 1 ppm Au-NP, 5 ppm Ag-NP, 60 ppm ZnO-NP, and 42.5 ppm ClO_2 .

The individual metal nanoparticles were synthesized according to the patented method.¹⁵ In brief, metal aqueous solutions such as chloroauric acid (HAuCl_4), silver nitrate (AgNO_3), zinc chloride (ZnCl_2) or selenium chloride (SeCl_4) were reduced by heating with citric acid or glucose at 150 °C for 12 min, and then dispersed in an appropriate medium to obtain the colloidal metal nanoparticles. According to the transmission electron microscopy imaging, Ag-NP, Se-NP, Au-NP, and ZnO-NP were in spherical shape with 10–40, 30–100, 20–40, and 25–35 nm diameters, respectively. Colloidal solutions of nanoparticle composite, namely ND50, NK99, and TPNT1 were prepared by well mixing of the above-described materials. The combination of Ag-NP and Au-NP had been shown synergistic antibacterial effect against *S. aureus* in the *in vitro* study.^{16,17} The addition of ZnO-NP and ClO_2 was based on their *in vitro* antibacterial effect.^{18–20}

Susceptibility tests and detection of carbapenemase-encoding genes

The MICs of each bacterial isolate to metal nanoparticle solutions were determined by broth microdilution according to Clinical Laboratories Standards Institute (CLSI) guidelines.²¹ In brief, the concentrated stock solutions of Ag-NP and Se-NP were diluted in the concentration of 100 ppm and then in the two-fold serial dilution. The nanoparticle composites ND50, NK99, and TPNT1 were prepared in the two-fold serial dilutions from stock solution provided by Tripod Nano Technology Corp (Taoyuan, Taiwan). Next, 0.1 (± 0.02) mL of broth containing different concentrations of colloidal metal nanoparticles were added to each well. Bacteria isolates in the standard density of 5×10^5 CFU/mL were then be inoculated to the panels, and the panels were incubated for 16–20 h at 35 ± 2 °C for visual determination of MICs. The susceptibility to other antibiotics were determined with VITEK 2 Automated System (BioMérieux, Marcy l'Etoile, France), except the susceptibility of *H. influenzae* to amoxicillin and clavulanate, ampicillin, cefuroxime, cefotaxime, cefixime, and trimethoprim/sulfamethoxazole were determined by disk diffusion test. The U.S. Food and Drug Administration tigeicycline breakpoint criteria for *Enterobacteriaceae* were used for both CRKP and CRAB. Isolates with an MIC ≤ 2 $\mu\text{g}/\text{mL}$ were considered as susceptible.²² The testing results of

the other antibiotics were interpreted according to the CLSI criteria.²¹ All CRKP isolates were subjected to multiplex polymerase chain reaction (PCR) detection of genes encoding carbapenemases, including *bla*_{KPC}, *bla*_{NDM}, and *bla*_{OXA-48}, using previously described methods.^{23,24} Clustering analysis of antibiogram types of each bacterial species were performed using the Ward's clustering method. The MIC values or the diameters of the inhibition zones determined in the antimicrobial sensitivity assay were used as the variables in clustering analysis. The correlations among isolates were expressed as the square of the Euclidean distance, and the results were displayed as a tree diagram. The clustering analysis of antibiograms were performed using SPSS software version 25.0 (IBM Corp. Armonk).

Results

Fifty each of CRAB, CRKP, *P. aeruginosa*, *H. influenzae*, *S. pneumoniae*, and MRSA isolates were included for analysis. Among 50 CRKP isolates, 27 (54%) were carbapenemase-producing *K. pneumoniae* (CPKP), including 26 KPC and one OXA-48. The cluster analysis of antibiogram types identified more than one cluster among each bacterial species, which indicated that these bacteria might be different clones (data not shown). The MIC values and antimicrobial susceptibilities of CRAB, CRKP, and *P. aeruginosa* isolates are provided in Table 1. All CRAB isolates had a colistin MIC ≤ 2 $\mu\text{g}/\text{mL}$, and 80% of them had a tigeicycline MIC ≤ 2 $\mu\text{g}/\text{mL}$. The susceptible rates of CRAB to other tested antibiotics were low. The susceptible rates of CRKP to amikacin and tigeicycline were 92% and 58%, respectively, and that to other tested antibiotics were less than 30%. Thirty-four (68%) of 50 CRKP isolates had a colistin MIC ≤ 2 $\mu\text{g}/\text{mL}$. The susceptible rates of *P. aeruginosa* isolates to aminoglycosides and fluoroquinolones were the highest (90%–100%), followed by third- or fourth-generation cephalosporin (80%–90%) and piperacillin/tazobactam (60%–70%). Seventeen (34%) of 50 *P. aeruginosa* isolates were CRPA.

The MIC₅₀s of Ag-NP for CRAB, CRKP, and *P. aeruginosa* were <3.125 ppm, 25 ppm, and <3.125 ppm, respectively. On the contrary, the MIC₅₀s of Se-NP for these three species of isolates were all >50 ppm (Fig. 1). Among CRAB, CRKP and *P. aeruginosa*, the MIC₅₀s of ND50, NK99, and TPNT1 for CRAB were the lowest (1/8 dilution, 1/8 dilution, and 1/8 dilution, respectively), while that for CRKP (>1/2 dilution, 1/2 dilution, and 1/2 dilution, respectively) and *P. aeruginosa* (>1/2 dilution, 1/4 dilution, 1/2 dilution, respectively) were higher. Compared with CRKP without production of carbapenemases (non-CPKP), the MIC₅₀ of Ag-NP for CPKP was higher (25 ppm vs. 50 ppm). However, the MIC₅₀s of ND50, NK99, and TPNT1 for CPKP and non-CPKP were the same (Supplementary Fig. 1). The distribution of the MICs of ND50, NK99, and TPNT1 between CSPA and CRPA were similar (Fig. 2).

Table 2 shows the susceptibility of 50 *H. influenzae* isolates to antimicrobials and tested nanoparticles. These *H. influenzae* isolates were highly susceptible to amoxicillin/clavulanate and cephalosporins. The MIC₅₀s of Ag-NP

Table 1 Antimicrobial susceptibility distributions of carbapenem-resistant *A. baumannii* (CRAB), carbapenem-resistant *K. pneumoniae* isolates (CRKP), and *P. aeruginosa*.

Antimicrobial agents	CRAB (n = 50)				CRKP (n = 50)				<i>P. aeruginosa</i> (n = 50)			
	MICs			S (%)	MICs			S (%)	MICs			S (%)
	Range	MIC ₅₀	MIC ₉₀		Range	MIC ₅₀	MIC ₉₀		Range	MIC ₅₀	MIC ₉₀	
Amikacin					≤2–≥64	≤2	16	92	≤2–16	≤2	8	100
Gentamicin	≤1–≥16	≥16	≥16	18	≤1–≥16	≥16	≥16	24	≤1–≥16	≤1	6	90
Cefepime	2–≥64	≥64	≥64	2	≤1–≥64	≥64	≥64	24	≤1–≥64	2	24	84
Ceftazidime	2–≥64	≥64	≥64	2	≤1–≥64	≥64	≥64	8	≤1–≥64	4	≥64	82
Ampi/Sul	≤2–≥32	≥32	≥32	2	≥32–≥32	≥32	≥32	0				
Pip/Tazo	≥128–≥128	≥128	≥128	0	≥128	≥128	≥128	2	≤4–≥128	8	≥128	68
Imipenem	8–≥16	≥16	≥16	0	0.5–≥16	≥16	≥16	0	≤0.25–≥16	2	≥16	66
Meropenem	8–≥16	≥16	≥16	0	≤0.25–≥32	≥16	≥16	6	≤0.25–≥16	0.375	16	70
Ciprofloxacin	≤0.25–≥4	≥4	≥4	4/49	≤0.25–≥4	≥4	≥4	16	≤0.25–≥4	≤0.25	0.75	92
Levofloxacin	≤0.12–≥8	≥8	≥8	5/49	≤0.12–≥8	≥8	≥8	16	≤0.12–≥8	0.5	2	92
Colistin	≤0.5–1	≤0.5	≤0.5	100 ^a	≤0.5–≥16	≤0.5	≥16	68 ^a	≤0.5–2	≤0.5	2	100 ^a
Tigecycline	≤0.5–≥8	2	4	80	≤0.5–≥128	2	≥8	58				
Nanoparticle												
Ag-NP	<3.125–<3.125	<3.125	<3.125	NA	<3.125–>50	25	>50	NA	<3.125–50	<3.125	<3.125	NA
Se-NP	>50–>50	>50	>50	NA	>50–>50	>50	>50	NA	>50–>50	>50	>50	NA
ND50	1/8–1/4	1/8	1/4	NA	>1/2–>1/2	>1/2	>1/2	NA	1/8–>1/2	>1/2	>1/2	NA
NK99	1/8–1/2	1/8	1/4	NA	1/16–>1/2	1/2	>1/2	NA	1/8–1/2	1/4	3/8	NA
TPNT1	1/8–1/4	1/8	3/16	NA	1/2–>1/2	1/2	>1/2	NA	1/16–1/2	1/2	1/2	NA

^a The percentages represent isolates with a colistin MIC ≤ 2 µg/ml

Note: The MICs are expressed in ppm for Ag-NP and Se-NP, in fold of dilution for ND50, NK99, TPNT1, and in µg/mL for other antibiotics. Abbreviations: Ag-NP, silver nanoparticles; Ampi/Sul, ampicillin/sulbactam; MIC, minimum inhibitory concentration; NA, not applicable; Pip/Tazo, piperacillin/tazobactam; S, susceptible; Se-NP, selenium nanoparticles.

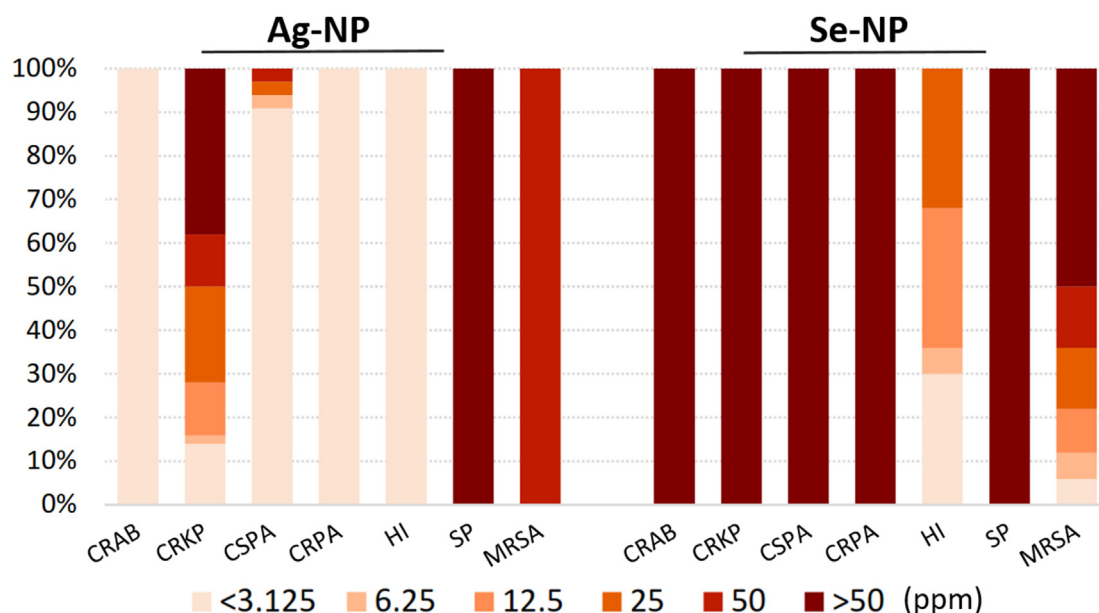


Figure 1. MIC distributions for silver nanoparticles (Ag-NP) and selenium nanoparticles (Se-NP) against carbapenem-resistant *A. baumannii* (CRAB, n = 50), carbapenem-resistant *K. pneumoniae* isolates (CRKP, n = 50), carbapenem-susceptible and -resistant *P. aeruginosa* (CSPA, n = 33, and CRPA, n = 17), *H. influenzae* (HI, n = 50), methicillin-resistant *S. aureus* (MRSA, n = 50), and *S. pneumoniae* (SP, n = 50) isolates.

and Se-NP were <3.125 ppm and 12.5 ppm, respectively. Among the six species evaluated for Se-NP, *H. influenzae* was the most susceptible one (Fig. 1). The MICs of ND50 and

NK99 for *H. influenzae* were all >1/2 dilution. The MIC₅₀ and MIC₉₀ of TPNT1 for *H. influenzae* were both 1/4 dilution.

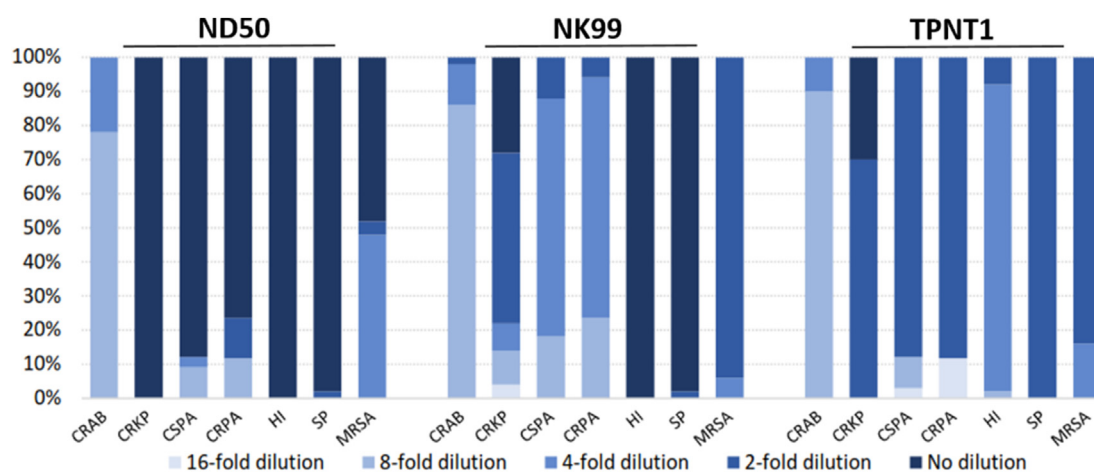


Figure 2. MIC distributions for ND50, NK99, TPNT1 against carbapenem-resistant *A. baumannii* (CRAB, $n = 50$), carbapenem-resistant *K. pneumoniae* isolates (CRKP, $n = 50$), carbapenem-susceptible and -resistant *P. aeruginosa* (CSPA, $n = 33$, and CRPA, $n = 17$), *H. influenzae* (HI, $n = 50$), *S pneumoniae* (SP, $n = 50$), and methicillin-resistant *S. aureus* (MRSA, $n = 50$) isolates.

Table 2 Susceptibility of *H. influenzae* isolates to antimicrobials and nanoparticles.

<i>H. influenzae</i> ($n = 50$)			
Antimicrobial agent	Susceptibility, n/n (%)		
Amoxi/Clavu	47/50 (94)		
Ampicillin	18/50 (36)		
Cefuroxime	49/50 (98)		
Cefotaxime	50/50 (100)		
Cefixime	50/50 (100)		
TMP/SMX	20/47 (42.6)		
Nanoparticles	MIC range	MIC ₅₀	MIC ₉₀
Ag-NP	<3.125–<3.125	<3.125	<3.125
Se-NP	<3.125–25	12.5	25
ND50	1/4–>1/2	>1/2	>1/2
NK99	>1/2–>1/2	>1/2	>1/2
TPNT1	1/8–1/2	1/4	1/4

Note: The MICs are expressed in ppm for Ag-NP and Se-NP, in fold of dilution for ND50, NK99, TPNT1, and in $\mu\text{g}/\text{mL}$ for other antibiotics.

Abbreviations: Ag-NP, silver nanoparticles; Amoxi/Clavu, amoxicillin/clavulanate; MIC, minimum inhibitory concentration; Se-NP, selenium nanoparticles; TMP/SMX, trimethoprim/sulfamethoxazole.

The antimicrobial susceptibilities of MRSA and *S. pneumoniae* were shown in Table 3. All MRSA isolates were susceptible to vancomycin, daptomycin, and linezolid, and 96% and 75% of them were susceptible to fusidic acid and trimethoprim/sulfamethoxazole, respectively. The susceptible rates of MRSA to clindamycin (63%) and levofloxacin (46%) were lower. The *S. pneumoniae* isolates were highly susceptible to vancomycin, levofloxacin, and moxifloxacin, but only 56% of isolates were susceptible to cefotaxime by non-meningitis criteria. For MRSA, all metal nanoparticle solutions showed high MICs. The MIC₅₀s of Ag-NP, Se-NP, ND50, NK99, and TPNT1 were 50 ppm, >50 ppm, >1/2 dilution, 1/2 dilution, and 1/2 dilution, respectively. *S.*

pneumoniae showed higher MICs of nanoparticle solutions compared to MRSA. The MIC₅₀s of Ag-NP, Se-NP, ND50, NK99, and TPNT1 for *S. pneumoniae* were >50 ppm, >50 ppm, >1/2 dilution, >1/2 dilution, and 1/2 dilution, respectively (Figs. 1 and 2).

Discussion

This study demonstrated that metal nanoparticles had greater *in vitro* activity against Gram-negative than Gram-positive bacteria. Of carbapenem-resistant Gram-negative bacteria, CRAB was the most susceptible, whereas CRKP was the least susceptible to metal nanoparticles. The MICs of Ag-NP for CRAB, CRKP, and *P. aeruginosa* were lower than that of Se-NP (MIC₅₀ <3.125 ppm, 25 ppm, <3.125 ppm vs. all >50 ppm). Among three nanoparticle composites, NK99 had the lowest MICs for *P. aeruginosa* when compared to ND50 and TPNT1 (MIC₅₀ 1/4 dilution vs. >1/2 dilution and 1/2 dilution).

Our results indicated that Ag-NP possessed great potential to inhibit the growth of drug-resistant Gram-negative bacteria. Silver was an inherently antibacterial material, and Ag-NP was considered the most toxic to bacteria among various metal nanoparticles.²⁵ The *in vitro* study conducted by Yang et al. showed Ag-NPs confined to mesostructured materials could induce a time-dependent accumulation of ROS and express antibacterial activity against CRKP,¹² which also supported the use of Ag-NP against carbapenem-resistant *Enterobacteriaceae*. In our study, the MICs of nanoparticles for Gram-negative bacteria were lower than that for Gram-positive bacteria. Likewise, Yuan et al. reported that Ag-NP exhibited dose- and time-dependent antibacterial effect, and its MICs for *P. aeruginosa* was lower than that for *S. aureus*.²⁶ This could be attributed to the thicker peptidoglycan cell wall of Gram-positive bacteria, which dampened the penetration of silver ions into cytoplasm.²⁷

Nanoparticle composites ND50, NK99, and TPNT1 were more effective against CRAB than CRKP and *P. aeruginosa* in our study. The reason for differences in the susceptibilities

Table 3 Antimicrobial susceptibility distributions of methicillin-resistant *S. aureus* (MRSA) and *S. pneumoniae* isolates.

Antimicrobial agent	MRSA (n = 50)				<i>S. pneumoniae</i> (n = 50)			
	MIC Range	MIC ₅₀	MIC ₉₀	S (%)	MIC Range	MIC ₅₀	MIC ₉₀	S (%)
Penicillin					≤0.06–≥8	2	4	68
Cefotaxime					≤0.12–≥8	1	4	56
Clindamycin	≤0.12–≥4	0.25	≥4	63	≤0.25–≥1	≥1	≥1	14
Erythromycin	≤0.25–≥8	≥8	≥8	38	≤0.12–≥8	≥8	≥8	8
Tetracycline	≤1–≥16	≤1	≥16	79	≤0.25–≥16	≥16	≥16	10
Vancomycin	≤0.5–2	1	1	100	≤0.12–0.5	0.5	0.5	100
Levofloxacin	≤0.12–≥8	4	≥8	46	≤0.25–≥16	0.5	1	94
Moxifloxacin					0.12–≥4	0.12	0.12	96
Ciprofloxacin	≤0.5–≥8	6	≥8	42				
Fusidic acid	≤0.5–≥32	≤0.5	≤0.5	96				
Daptomycin	0.25–1	0.5	1	100				
Linezolid	≤0.5–1	2	2	100				
TMP/SMX	≤10–≥320	≤10	≥320	75				
Nanoparticles								
Ag-NP	50–50	50	50	NA	>50–>50	>50	>50	NA
Se-NP	>50–>50	>50	>50	NA	>50–>50	>50	>50	NA
ND50	>1/2–>1/2	>1/2	>1/2	NA	1/2–>1/2	>1/2	>1/2	NA
NK99	1/4–1/2	1/2	1/2	NA	1/2–>1/2	>1/2	>1/2	NA
TPNT1	1/2–1/2	1/2	1/2	NA	1/2–1/2	1/2	1/2	NA

Note: The MICs are expressed in ppm for Ag-NP and Se-NP, in fold of dilution for ND50, NK99, TPNT1, and in µg/mL for other antibiotics. Abbreviations: Ag-NP, silver nanoparticles; MIC, minimum inhibitory concentration; NA, not applicable; S, susceptible; Se-NP, selenium nanoparticles; TMP/SMX, trimethoprim/sulfamethoxazole.

of drug-resistant Gram-negative bacteria to nanoparticles remains unclear. Studies suggested that the bacterial resistance to nanoparticles might be related to upregulation of efflux pumps and the change in permeability of outer membrane.^{28,29} However, the association between characteristics of outer membrane proteins and nanoparticle MICs of carbapenem-resistant bacteria needs further investigations. Among three nanoparticle composites, NK99 had better activity against *P. aeruginosa*, and it was different from ND50 and TPNT-1 in the lower concentrations of Au-NP and lack of ClO₂. Synergistic effects of silver-gold bimetallic nanoparticles had been shown, but the optimal proportion of each component has not been determined.¹⁷

Nanoparticles had been evaluated as inhaled therapy. In a clinical trial on 50 patients with laryngeal tuberculosis, Ag-NP inhalation therapy achieved higher rates of sputum clearance and laryngeal wound healing than standard anti-tuberculosis treatment.³⁰ However, toxicity was a concern. In animal study, Ag-NP accumulated in vital organs after inhaled exposure with systemic toxicity.³¹ Inhalation of ZnO-NP was also reported to reduce tidal-volume in mice and cause airway inflammation in human.^{32,33} The toxicity of nanoparticles were determined by their chemical composition, particle size, crystal structure, concentrations, and the rate of ion release.³⁴ In our study, the metal nanoparticles were produced in spherical shape, and nanospheres were shown to be less cytotoxic than nanorods.³⁵ Nevertheless, the safe dose range of metal nanoparticles had not been established. Another challenging issue is the emergence of resistance. Both chromosomal and plasmid-mediated resistance contributed to the

adaptation of bacteria to metal nanoparticles.³⁶ Experiments showed *E. coli* evolved rapidly to develop resistance within treatment of Ag-NPs,³⁷ and *S. aureus* acquired resistance by mutations on genes participated in oxidative stress defense and nucleotide synthesis.³⁸

There are several limitations in our study. First, only a small number of each species from a single center were tested. Subsequent multicenter study is warranted to validate our findings. Second, the number of CPKP isolates was limited. Therefore, the differences in the susceptibilities to nanoparticles between carbapenemase-producing and non-carbapenemase-producing strains might not be observed. Third, the toxicity of these nanoparticle solutions toward mammalian cells were not evaluated. It is unknown whether their antibacterial effects will remain at the safe dose for mammalian cells or when uptake through inhalation.

In conclusion, metal nanoparticles and nanoparticle composites showed good *in vitro* activity against Gram-negative bacteria, including drug-resistant strains. Among carbapenem-resistant Gram-negative bacteria, CRAB was the most susceptible to nanoparticles. Further research is needed to explore the potential application of nanoparticles and nanoparticle composites as environmental disinfectants or therapeutic agents for MDRO-related infections.

Ethics approval

This study was reviewed by the National Taiwan University Hospital Research Ethics Committee, and the need for approval was waived.

Consent for publication

Not applicable.

Availability of data and materials

All data generated or analyzed during this study are included in this published article and its supplementary information files.

Funding

This study was partially supported by Tripod Nano Technology Corporation. The sponsors had no role in the study design, data collection and analysis, manuscript preparation, or the decision to submit for publication.

Authors' contributions

YSH and JTW designed the study. YSH and HMT conducted experiments and analyzed the data. YSH performed statistical analyses and wrote the manuscript. JTW and PCY critically reviewed the manuscript. PCC and HCH provide supports for experiments. All authors read and approved the final manuscript.

Declaration of competing interest

None to declare.

Acknowledgements

Not applicable.

References

- Drijkoningen JJ, Rohde GG. Pneumococcal infection in adults: burden of disease. *Clin Microbiol Infect* 2014;20(Suppl 5):45–51.
- Liñares J, Ardanuy C, Pallares R, Fenoll A. Changes in antimicrobial resistance, serotypes and genotypes in *Streptococcus pneumoniae* over a 30-year period. *Clin Microbiol Infect* 2010;16(5):402–10.
- Rhodes NJ, Cruce CE, O'Donnell JN, Wunderink RG, Hauser AR. Resistance trends and treatment options in Gram-negative ventilator-associated pneumonia. *Curr Infect Dis Rep* 2018;20(2):3.
- Patel IS, Seemungal TA, Wilks M, Lloyd-Owen SJ, Donaldson GC, Wedzicha JA. Relationship between bacterial colonisation and the frequency, character, and severity of COPD exacerbations. *Thorax* 2002;57(9):759–64.
- Rodrigo-Troyano A, Sibila O. The respiratory threat posed by multidrug resistant Gram-negative bacteria. *Respirology* 2017;22(7):1288–99.
- Weber DJ, Rutala WA, Miller MB, Huslage K, Sickbert-Bennett E. Role of hospital surfaces in the transmission of emerging health care-associated pathogens: norovirus, *Clostridium difficile*, and *Acinetobacter* species. *Am J Infect Control* 2010;38(5 Suppl 1):S25–33.
- Kawamura-Sato K, Wachino J, Kondo T, Ito H, Arakawa Y. Reduction of disinfectant bactericidal activities in clinically isolated *Acinetobacter* species in the presence of organic material. *J Antimicrob Chemother* 2008;61(3):568–76.
- Horner C, Mawer D, Wilcox M. Reduced susceptibility to chlorhexidine in staphylococci: is it increasing and does it matter? *J Antimicrob Chemother* 2012;67(11):2547–59.
- Abdal Dayem A, Hossain MK, Lee SB, Kim K, Saha SK, Yang GM, et al. The role of reactive oxygen species (ROS) in the biological activities of metallic nanoparticles. *Int J Mol Sci* 2017;18(1).
- Lara HH, Guisbiers G, Mendoza J, Mimun LC, Vincent BA, Lopez-Ribot JL, et al. Synergistic antifungal effect of chitosan-stabilized selenium nanoparticles synthesized by pulsed laser ablation in liquids against *Candida albicans* biofilms. *Int J Nanomed* 2018;13:2697–708.
- Guisbiers G, Wang Q, Khachatryan E, Mimun LC, Mendoza-Cruz R, Larese-Casanova P, et al. Inhibition of *E. coli* and *S. aureus* with selenium nanoparticles synthesized by pulsed laser ablation in deionized water. *Int J Nanomed* 2016;11:3731–6.
- Yang TY, Hsieh YJ, Lu PL, Lin L, Wang LC, Wang HY, et al. In vitro and in vivo assessments of inspired Ag/80S bioactive nanocomposites against carbapenem-resistant *Klebsiella pneumoniae*. *Mater Sci Eng C* 2021;125:112093.
- Sharma R, Raghav R, Priyanka K, Rishi P, Sharma S, Srivastava S, et al. Exploiting chitosan and gold nanoparticles for antimycobacterial activity of in silico identified antimicrobial motif of human neutrophil peptide-1. *Sci Rep* 2019;9(1):7866.
- Deshmukh SP, Patil SM, Mullani SB, Delekar SD. Silver nanoparticles as an effective disinfectant: a review. *Materials science & engineering C, Materials for biological applications* 2019;97:954–65.
- Lin L, Fan KS, Wang CH, Chiu CL, Chang TW, Wang CD, et al. Method of making colloidal metal nanoparticles, USA patent US10099191B1. 2018. <https://patentimages.storage.googleapis.com/1c/cb/8b/a22ce49551b8a4/US10099191.pdf>.
- Kumar S, Majhi RK, Singh A, Mishra M, Tiwari A, Chawla S, et al. Carbohydrate-coated gold-silver nanoparticles for efficient elimination of multidrug resistant bacteria and in vivo wound healing. *ACS Appl Mater Interfaces* 2019;11(46):42998–3017.
- Bai MY, Ku FY, Shyu JF, Hayashi T, Wu CC. Evaluation of polyacrylonitrile nonwoven mats and silver-gold bimetallic nanoparticle-decorated nonwoven mats for potential promotion of wound healing in vitro and in vivo and bone growth in vitro. *Polymers (Basel)* 2021;13(4).
- Jin SE, Jin JE, Hwang W, Hong SW. Photocatalytic antibacterial application of zinc oxide nanoparticles and self-assembled networks under dual UV irradiation for enhanced disinfection. *Int J Nanomed* 2019;14:1737–51.
- Król A, Pomastowski P, Rafińska K, Railean-Plugaru V, Buszewski B. Zinc oxide nanoparticles: synthesis, antiseptic activity and toxicity mechanism. *Adv Colloid Interface Sci* 2017;249:37–52.
- Ma JW, Huang BS, Hsu CW, Peng CW, Cheng ML, Kao JY, et al. Efficacy and safety evaluation of a chlorine dioxide solution. *Int J Environ Res Publ Health* 2017;14(3):329.
- Wayne P. *Clinical and laboratory standards Institute (CLSI). Performance standards for antimicrobial susceptibility testing*. 29th ed. 2019. CLSI supplement M100.
- The US Food and Drug Administration (FDA) Identified interpretive criteria of tigecycline. FDA; 2019. <https://www.fda.gov/drugs/development-resources/tigecycline-injection-products>.
- Queenan AM, Bush K. Carbapenemases: the versatile beta-lactamases. *Clin Microbiol Rev* 2007;20(3):440–58. table of contents.
- Dortet L, Brécharde L, Cuzon G, Poirel L, Nordmann P. Strategy for rapid detection of carbapenemase-producing Enterobacteriaceae. *AAC (Antimicrob Agents Chemother)* 2014;58(4):2441–5.

25. Baptista PV, McCusker MP, Carvalho A, Ferreira DA, Mohan NM, Martins M, et al. Nano-strategies to fight multidrug resistant bacteria-"a battle of the titans. *Front Microbiol* 2018;**9**:1441.
26. Yuan YG, Peng QL, Gurunathan S. Effects of silver nanoparticles on multiple drug-resistant strains of staphylococcus aureus and pseudomonas aeruginosa from mastitis-Infected goats: an alternative approach for antimicrobial therapy. *Int J Mol Sci* 2017;**18**(3).
27. Tang S, Zheng J. Antibacterial activity of silver nanoparticles: structural effects. *Adv Healthc Mater* 2018;**7**(13):e1701503.
28. Lee NY, Ko WC, Hsueh PR. Nanoparticles in the treatment of infections caused by multidrug-resistant organisms. *Front Pharmacol* 2019;**10**:1153.
29. Finley PJ, Norton R, Austin C, Mitchell A, Zank S, Durham P. Unprecedented silver resistance in clinically isolated Enterobacteriaceae: major implications for burn and wound management. *Antimicrob Agents Chemother* 2015;**59**(8):4734–41.
30. Uraskulova BB, Gyusan AO. [The clinical and bacteriological study of the effectiveness of the application of silver nanoparticle for the treatment of tuberculosis]. *Vestn Otorinolaringol* 2017;**82**(3):54–7.
31. Nayek S, De Silva IW, Aguilar R, Lund AK, Verbeck GF. Toxicological alterations induced by subacute exposure of silver nanoparticles in Wistar rats. *J Appl Toxicol* 2021;**41**(6): 972–86.
32. Jacobsen NR, Stoeger T, van den Brule S, Saber AT, Beyerle A, Vietti G, et al. Acute and subacute pulmonary toxicity and mortality in mice after intratracheal instillation of ZnO nanoparticles in three laboratories. *Food Chem Toxicol* 2015;**85**: 84–95.
33. Monsé C, Raulf M, Hagemeyer O, van Kampen V, Kendzia B, Gering V, et al. Airway inflammation after inhalation of nano-sized zinc oxide particles in human volunteers. *BMC Pulm Med* 2019;**19**(1):266.
34. Quadros ME, Marr LC. Environmental and human health risks of aerosolized silver nanoparticles. *J Air Waste Manag Assoc* 2010;**60**(7):770–81.
35. Schaeublin NM, Braydich-Stolle LK, Maurer EI, Park K, MacCuspie RI, Afroz AR, et al. Does shape matter? Bioeffects of gold nanomaterials in a human skin cell model. *Langmuir* 2012;**28**(6):3248–58.
36. McNeilly O, Mann R, Hamidian M, Gunawan C. Emerging Concern for Silver Nanoparticle resistance in acinetobacter baumannii and other bacteria. *Front Microbiol* 2021;**12**: 652863.
37. Graves Jr JL, Tajkarimi M, Cunningham Q, Campbell A, Nonga H, Harrison SH, et al. Rapid evolution of silver nanoparticle resistance in Escherichia coli. *Front Genet* 2015;**6**:42.
38. Valentin E, Bottomley AL, Chilambi GS, Harry EJ, Amal R, Sotiriou GA, et al. Heritable nanosilver resistance in priority pathogen: a unique genetic adaptation and comparison with ionic silver and antibiotics. *Nanoscale* 2020;**12**(4):2384–92.

Appendix A. Supplementary data

Supplementary data to this article can be found online at <https://doi.org/10.1016/j.jmii.2022.05.003>.